Chip-Based Resonance Raman Spectroscopy Using Tantalum Pentoxide Waveguides

David A. Coucheron, Dushan N. Wadduwage, G. Senthil Murugan, Peter T. C. So, and Balpreet S. Ahluwalia

***Abstract*— Blood analysis is an important diagnostic tool, as it provides a wealth of information about the patient's health. Raman spectroscopy is a promising tool for blood analysis, but widespread clinical application is limited by its low signal strength, as well as complex and costly instrumentation. The growing field of waveguide-based Raman spectroscopy tries to solve these challenges by working toward fully integrated Raman sensors with increased interaction areas. In this letter, we demonstrate resonance Raman measurements of hemoglobin, a crucial component of blood, at 532-nm excitation using a tantalum pentoxide (Ta_2O_5) waveguide platform. We have also characterized the background signal from Ta_2O_5 waveguide material when excited at 532 nm. In addition, we demonstrate spontaneous Raman measurements of isopropanol and methanol using the same platform. Our results suggest that Ta_2O_5 is a promising waveguide platform for resonance Raman spectroscopy at 532 nm and, in particular, for blood analysis.**

***Index Terms*— Optical waveguides, Raman scattering, photonic integrated circuits, biosensors.**

I. Introduction

BLOOD is an essential bodily fluid that consists mainly of red blood cells, white blood cells and platelets in a liquid medium called plasma. The components of blood serve different purposes, ranging from oxygen transport to fighting disease and infection. Analyses of blood can thus give vital insight into a person's health and can identify diseases such as diabetes, malaria and sickle-cell disease [1]. Hemoglobin, the major component of red blood cells, has been of interest in the Raman spectroscopy community since the 1970s [2], as it dominates the Raman spectrum of blood. Spontaneous Raman scattering has a very low scattering cross-section and is thus a weak effect. Hemoglobin, however, experiences resonance Raman at 532 nm excitation, enhancing the signal significantly [2]. The widespread application of Raman spectroscopy in routine clinical analysis is, however, limited by e.g. low throughput, complex and costly instrumentation [3].

On-chip Raman spectroscopy [4] using integrated optical waveguides is an attractive route for delivering compact, simple to operate, affordable and highly sensitive Raman spectrometers. The main reason is that the use of waveguides offers a simple way to increase the Raman scattering, as well as the possibility of a fully integrated sensor on chip, making instrumentation far simpler.

Raman spectroscopy using waveguides made of high-refractive index contrast (HIC) materials is experiencing a renewed interest [5]–[8]. Recent achievements include measurements of biological monolayers [9] and trace gases [10]. When light is guided in an optical waveguide, an evanescent field is generated outside the waveguide core, which can be used to probe a sample close to the waveguide surface. Raman scattering from the sample will either recouple into the waveguide or emit into free space (as illustrated in Fig. 1a by the orange arrows). Detection can therefore be done either from the top of the waveguide or from the end facet of the waveguide-chip, as illustrated in Fig.1b. This technique is commonly called waveguide enhanced Raman spectroscopy (WERS) when detection is done from the end, as the waveguide structure gives rise to intrinsic enhancement effects for thin samples (e.g. monolayers). Waveguides made of HIC materials benefit from two enhancement effects when using edge detection for thin samples: 1) Radiative enhancement due to the high intensity of the evanescent field and 2) interaction area enhancement due to the increased

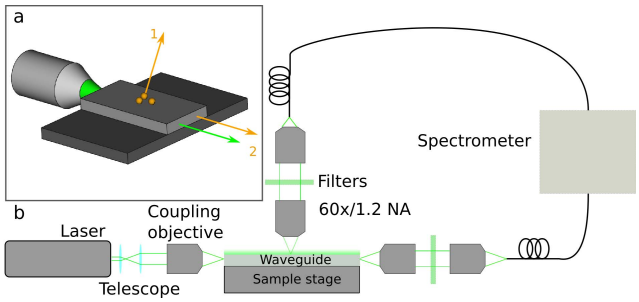

Fig. 1. (a) Illustration of Raman scattering from a sample on a waveguide. The evanescent field can induce Raman scattering in a sample. The scattered photons can either be transmitted into free space (1) or recoupled back into the waveguide (2). (b) Schematic of the system used in the experiments.

Manuscript received February 21, 2019; revised April 6, 2019; accepted April 30, 2019. Date of publication May 8, 2019; date of current version June 25, 2019. This work was supported in part by the European Research Council under Project 336716 and in part by The Arctic University of Norway (UiT) through the Tematiske satsinger. *(Corresponding author: Balpreet S. Ahluwalia.)*

D. A. Coucheron and B. S. Ahluwalia are with the Department of Physics and Technology, The Arctic University of Norway (UiT), 9019 Tromsø, Norway (e-mail: balpreet.singh.ahluwalia@uit.no).

D. N. Wadduwage is with the Laser Biomedical Research Center, Massachusetts Institute of Technology, Cambridge, MA 02139 USA, also with the Department of Biological Engineering, Massachusetts Institute of Technology, Cambridge, MA 02139 USA, and also with the Center for Advanced Imaging, Harvard University, Cambridge, MA 02138 USA.

G. S. Murugan is with the Optoelectronics Research Centre, University of Southampton, Southampton SO17 1BJ, U.K.

P. T. C. So is with the Laser Biomedical Research Center, Massachusetts Institute of Technology, Cambridge, MA 02139 USA, and also with the Department of Biological Engineering, Massachusetts Institute of Technology, Cambridge, MA 02139 USA.

Color versions of one or more of the figures in this letter are available online at http://ieeexplore.ieee.org.

Digital Object Identifier 10.1109/LPT.2019.2915671

interaction area [6]. The HIC material tightly confines the light within the waveguide core, enabling ultra-small footprints of the optical functions. If the propagation loss is low, arbitrarily large interaction areas can be designed through e.g. a spiral geometry [5]. The instrumentation can also be made much simpler, as a waveguide based set-up can have integrated lasers [11], detectors [12] and other components needed for Raman spectroscopy.

Most of the recent result on waveguide based Raman spectroscopy has been performed using silicon nitride (Si_3N_4) nanowires [5] and slot waveguides [13] with 785 nm excitation light. The increased field intensity inside the slot can give a fivefold or more increase in signal strength [14]. Spiral slot waveguides are highly sensitive and have been used to measure biological sub-monolayers [9]. Despite the success of Si_3N_4 spiral waveguides, getting sufficient Raman scattering without cooled detectors, which is relevant for a fully integrated solution, remains challenging. Several approaches have been taken to improve the signal further in combination with the waveguide platform. One interesting approach is to use surface enhanced Raman scattering (SERS), which can give a signal increase of many orders of magnitude. Several approaches have been studied for SERS implementation, including the use of nanoporous gold [15] and gold bow-tie antenna [16]. A challenge with SERS is that it requires surface treatments that can generate hot spots and reduce life-time. Recently, metallic slot waveguides [17] and stimulated Raman scattering [8] approach were proposed. Another promising option for increasing the Raman signal, is by moving to lower wavelengths, as Raman scattering scales with λ^{-4}. Lower wavelengths can, however, also increase any auto-fluorescence background, which is usually much higher than the signals from Raman scattering. If the material background at lower wavelength is mainly from the Raman scattering, and not auto-fluorescence, it should not be a problem though. An additional advantages of lower excitation wavelength is possible resonance effects for selective samples. Resonance Raman occurs for certain samples at low wavelengths and can enhance the signal by several orders of magnitude. Using 532 nm excitation is particularly interesting due to resonance Raman effects in several clinically relevant samples, such as hemoglobin [2] and in cancerous brain [18] and breast tissue [19]. Taking advantage of resonance Raman effects can be key to really bring e.g. Raman based blood analysis to the market.

The development of HIC waveguide platform for resonance Raman spectroscopy using 532 nm excitation is therefore beneficial. Evans et al. have recently demonstrated waveguide based Raman spectroscopy using a TiO_2 platform at 532 nm excitation [7]. Another potential platform for shorter wavelength excitation is Ta_2O_5. Ta_2O_5 is a promising waveguide material for Raman spectroscopy due to its high refractive index contrast with silica cladding, providing strong optical mode confinement and thereby enabling the development of compact photonic circuits with tight bends and spirals. Ta_2O_5 is CMOS compatible and mass-producible, and offers a wide transparency window with UV absorption band edge below 330 nm and has been widely used in sensing applications [20]. Wang et al. have demonstrated both edge and top detection using Ta_2O_5 waveguides with 638 nm excitation [6], however, resonance Raman using 532 nm has yet to be investigated for biological application.

In this work, we present waveguide-based Raman spectroscopy using Ta_2O_5 waveguides using 532 nm excitation. We demonstrate spontaneous Raman spectroscopy of isopropanol and methanol. The background signal from the waveguide platform is investigated by changing the under cladding material between silicon dioxide (SiO_2) and magnesium fluoride (MgF_2). Finally, we measure resonance Raman spectrum of hemoglobin, suggesting the potential of Ta_2O_5 waveguide-based Raman spectroscopy platform for biological applications.

II. Set-Up and Waveguide Fabrication

A 532 nm laser (Verdi V10) was used for all experiments. The laser was coupled into the waveguides using a 0.5 N.A. aspheric lens on a three-axis piezo stage. Collection was done from the top using a 60x/1.2 NA WI objective lens (Olympus), unless otherwise stated. All work was performed with top collection, as we aim to use the spatial information for Raman imaging in future work. The emission light was relayed through two 532 nm edge filters (Semrock RazorEdge) and coupled into a multimode fiber. A spectrograph (Andor Holospec-F/1.8-VIS) was used to analyze the signal coupled out of the fiber. A schematic of the set-up used is presented in Figure 1b. All sample measurements were done using Ta_2O_5 strip waveguides on oxidized silicon (Si) wafers. The optimization of the fabrication process is described in previous work [21].

High-intensity in the evanescent field is desirable for on-chip Raman spectroscopy. This was achieved by fabricating thin, (150 nm) Ta_2O_5 materials in stripe geometry. The waveguide width ranges from 2.5 to 70 μm. The wide waveguides were investigated because our future aim is to use wide waveguides for Raman imaging, and thus requiring excitation of large areas. For the chosen waveguide dimensions up to 10% of the guided power was present in the evanescent field for 532 nm wavelength. The waveguides were originally fabricated for longer wavelengths and we found a relatively high propagation loss at 532 nm excitation of approximately 5 dB/cm and a coupling loss of approximately 11 dB.

Additionally, Ta_2O_5 waveguides were fabricated on MgF_2 substrates to study the background signal from the under-cladding material. Strip waveguides with different widths were defined in the Ta_2O_5 layer using standard photolithography and etched by 150 nm using argon ion beam milling. Finally, the waveguide samples were annealed at 600 °C for 3 hours under an oxygen atmosphere to relieve any stress built up in the films [22] and to replenish the oxygen, which is depleted during the sputtering process. 2.5 μm wide Ta_2O_5 waveguides on SiO_2 and on MgF_2 were used for the measurement. Prior to measurements, the waveguides were cleaned for 10 minutes in 1% Hellmanex in deionized (DI) water at 70 °C. The sample was then added in the hollow rectangular PDMS chamber and a cover slip was used to seal it.

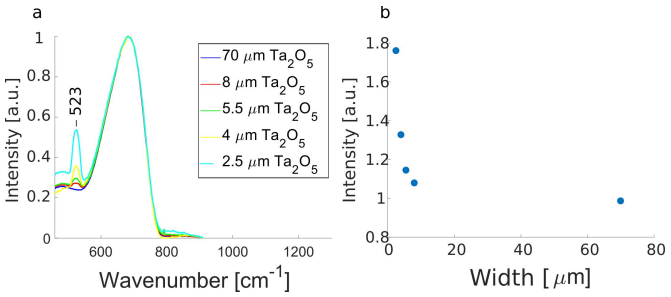

Fig. 2. (a) Normalized spectra measured as a function of waveguide width. (b) The ratio of the emerging peak at 523 cm^{-1} to the largest peak at 680 cm^{-1} as a function of waveguide width. The spectra are normalized to the widest waveguide.

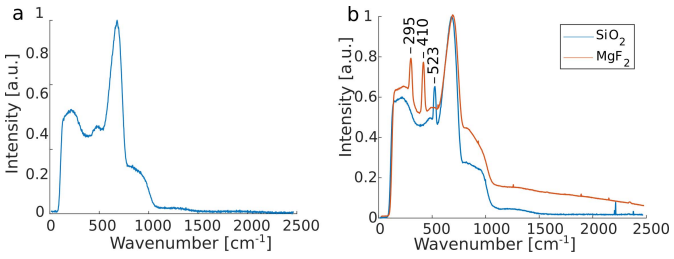

Fig. 3. (a) Background spectrum from a 70 μm wide Ta_2O_5 strip waveguide on a SiO_2 undercladding. (b) Background spectrum from 2.5 μm wide Ta_2O_5 waveguides on a SiO_2 and MgF_2 undercladding.

III. Background Measurements

First, we measured the background spectrum of Ta_2O_5 waveguides. The measurements were done with a 70 μm wide Ta_2O_5 strip waveguide. A laser beam (38 mW power) was incident at the input facet of the waveguide. Measurements were taken using a 20 s exposure time. The resulting spectra were normalized with respect to the highest peak at approximately 680 cm^{-1} and is presented in Figure 3a. Ta_2O_5 only exhibits a background signal from wavenumbers shorter than approximately 1000 cm^{-1}. Four peaks can be discerned: a large peak at 680 cm^{-1}; two smaller peaks at 488 cm^{-1} and 196 cm^{-1}; and a shoulder at 899 cm^{-1}. This agrees well with previous literature on amorphous Ta_2O_5 [22]. For peaks above 1000 cm^{-1}, most of the background can thus be filtered out.

We measured the background spectrum for Ta_2O_5 strip waveguides of different widths (2.5-70 μm) as shown in Fig. 2. The signal strength changed significantly for the different waveguide widths, as both coupling and propagation loss depends on the waveguide geometry. The overall spectrum shape, however, remained unchanged as the waveguide width was changed, but a new peak emerged at approximately 523 cm^{-1} for the narrower waveguides, which is typical Si-Si peak, originating from under-cladding. The spectra are thus normalized internally to the 680 cm^{-1} peak for each width. Fig. 2b presents the ratio of the peaks at 523 cm^{-1} to the local background level at 485 cm^{-1}, normalized for the ratio obtained using 70 μm wide waveguide. With decreasing width, the ratio increases rapidly below approximately 5 μm. For thinner waveguides, signals from the under-cladding becomes more prominent. For thin (150 nm) and narrow waveguides (<5 μm), the guided mode stretches further outside the core into the cladding, resulting in small contribution from the cladding. The results suggest that most of the overall spectral signal is from the Ta_2O_5 core and not the under-cladding for wide waveguides.

To further investigate the signal originating from the under-cladding, we compared Ta_2O_5 waveguides fabricated with two different under-claddings: silicon dioxide (SiO_2) and magnesium fluoride (MgF_2). Narrow Ta_2O_5 strip waveguide of 2.5 μm width were measured for two under-claddings, SiO_2 and MgF_2. A laser beam with 110 mW power was incident at the input facet of the waveguides and 10 s exposure time was used. The spectrum was averaged over 10 measurements to reduce the noise. The resulting spectra are presented in Fig. 3. The general shape of the spectrum remains unchanged, suggesting that the waveguide material contributes to most of the background signal. There are, however, a few notable changes. The sharp peak at 523 cm^{-1} from the Ta_2O_5 on SiO_2 is replaced with two new peaks at 410 cm^{-1} and 295 cm^{-1} for the Ta_2O_5 on MgF_2. The peaks at 410 cm^{-1} and 295 cm^{-1} are confirmed to be Raman peaks from MgF_2 [23]. The small peak at around 2250 cm^{-1} is a cosmic ray signal. Reducing the background further is thus challenging, since the background signal is dominated by the waveguide material and cannot easily be changed. It might, however, be possible to reduce the background by changing the fabrication process and a more detailed study into the origin of the signal in the Ta_2O_5 structure is needed.

IV. Waveguide Raman Measurements

Spontaneous Raman measurements of methanol and isopropanol with 532 nm excitation were performed using 150 nm thick Ta_2O_5 strip waveguides. The waveguides were 70 μm wide to increase the sensing area. A laser beam of 395 mW power was launched from the coupling objective. Both isopropanol and methanol were measured using a PDMS chamber to hold the sample, sealed with a cover glass. An exposure time of 20 s was used for both the samples. The presented spectrum is the average over three measurements. Spectra for methanol and isopropanol using waveguide excitation are presented in Fig. 4a. The waveguide background has been subtracted and all spectra have been normalized to the 822 cm^{-1} peak for isopropanol and the 890 cm^{-1} peak for methanol. The peaks agree well with literature [24] and the two chemicals are easily distinguishable by e.g. the symmetric C-O-O vibration at 822 and 890 cm^{-1} for isopropanol and methanol, respectively.

A motivation for using 532 nm excitation is to measure resonance Raman signals from hemoglobin, as it is important in lab-on-a-chip blood analysis for point of care diagnosis. Resonance Raman can distinguish different hemoglobin derivatives accurately [2]. For hemoglobin resonance Raman we used human hemoglobin (lyophilized powder from Sigma Aldrich) with 15.5 mM concentration in distilled water, which is similar to the hemoglobin concentration in red blood cells [25]. A drop was placed on the waveguide surface and allowed to dry. Collection was done with a 40x/0.75 NA air objective lens for this experiment, with 2 s exposure time.

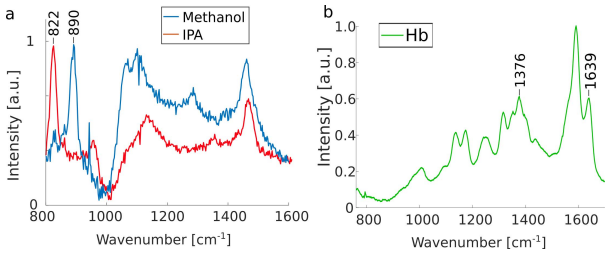

Fig. 4. (a) Spontaneous Raman spectra of methanol and isopropanol (IPA). (b) Resonance Raman spectrum of dried hemoglobin (Hb).

Fig. 4b shows the resonant Raman spectrum of dried hemoglobin. The presence of peaks at 1639 cm^{-1} and 1376 cm^{-1} demonstrates that the sample is oxygenated [1]. The Raman peaks are mostly above 1000 cm^{-1}, therefore, they are not overlapping with the waveguide background. This makes Ta_2O_5 ideally suited for resonance Raman spectroscopy for hemoglobin and blood analysis for point of care diagnostics. Here, we have employed only straight strip waveguides and top detection. The sensitivity can be further increased by changing to a spiral loop geometry and by doing edge detection, which will be explored in future work. The long-term goal is, however, to make use of spatial information of individual red blood cells either by performing optical imaging and/or Raman imaging using waveguide excitation. As such, optimizing wide waveguides for Raman spectroscopy are of interest.

V. Conclusion

Photonic integrated circuits provide a promising approach to Raman spectroscopy. Ta_2O_5 waveguides with its low background signal and high refractive index contrast has been demonstrated as a suitable platform for resonance Raman spectroscopy at 532 nm. By investigating waveguides of different under-claddings it was found that most of the background comes from the Ta_2O_5 core and only a small background from the surrounding media is visible for narrow waveguides. We have tested and validated the waveguide platform by measuring spontaneous Raman spectra of isopropanol and methanol. We have performed resonance Raman measurements of dried hemoglobin at concentration usually found in the red blood cells using the Ta_2O_5 waveguides. The resonance Raman spectroscopy can also be combined with other complementary optical functions developed using Ta_2O_5 material, such as optical nanoscopy [26], [27].

References

[1] C. G. Atkins, K. Buckley, M. W. Blades, and R. F. B. Turner, "Raman spectroscopy of blood and blood components," *Appl. Spectrosc.*, vol. 71, no. 5, pp. 767–793, 2017.

[2] T. C. Strekas and T. G. Spiro, "Hemoglobin: Resonance Raman spectra," *Biochim. Et Biophys. Acta (BBA) Protein Struct.*, vol. 263, no. 3, pp. 830–833, May 1972.

[3] I. Pence and A. Mahadevan-Jansen, "Clinical instrumentation and applications of Raman spectroscopy," *Chem. Soc. Rev.*, vol. 45, no. 7, pp. 1958–1979, Mar. 2016.

[4] A. Dhakal *et al.*, "Single mode waveguide platform for spontaneous and surface-enhanced on-chip Raman spectroscopy," *Interface Focus*, vol. 6, no. 4, Aug. 2016, Art. no. 20160015.

[5] A. Dhakal, A. Z. Subramanian, P. Wuytens, F. Peyskens, N. L. Thomas, and R. Baets, "Evanescent excitation and collection of spontaneous Raman spectra using silicon nitride nanophotonic waveguides," *Opt. Lett.*, vol. 39, no. 13, pp. 4025–4028, Jul. 2014.

[6] Z. Wang, M. N. Zervas, P. N. Bartlett, and J. S. Wilkinson, "Surface and waveguide collection of Raman emission in waveguide-enhanced Raman spectroscopy," *Opt. Lett.*, vol. 41, no. 17, pp. 4146–4149, Sep. 2016.

[7] C. C. Evans, C. Liu, and J. Suntivich, "TiO_2 nanophotonic sensors for efficient integrated evanescent Raman spectroscopy," *ACS Photon.*, vol. 3, no. 9, pp. 1662–1669, Sep. 2016.

[8] C. Zhang *et al.*, "Stimulated Raman scattering flow cytometry for label-free single-particle analysis," *Optica*, vol. 4, no. 1, pp. 103–109, Jan. 2017.

[9] A. Dhakal, P. C. Wuytens, F. Peyskens, K. Jans, N. L. Thomas, and R. Baets, "Nanophotonic waveguide enhanced Raman spectroscopy of biological submonolayers," *ACS Photon.*, vol. 3, no. 11, pp. 2141–2149, Nov. 2016.

[10] S. A. Holmstrom *et al.*, "Trace gas Raman spectroscopy using functionalized waveguides," *Optica*, vol. 3, no. 8, pp. 891–896, Aug. 2016.

[11] A. Aghajani, G. S. Murugan, N. P. Sessions, V. Apostolopoulos, and J. S. Wilkinson, "Waveguide lasers in ytterbium-doped tantalum pentoxide on silicon," *Opt. Lett.*, vol. 40, no. 11, pp. 2549–2552, Jun. 2015.

[12] H. Park *et al.*, "A hybrid AlGaInAs-silicon evanescent waveguide photodetector," *Opt. Express*, vol. 15, no. 10, pp. 6044–6052, 2007.

[13] A. Dhakal, F. Peyskens, A. Z. Subramanian, N. Le Thomas, and R. Baets, "Enhanced spontaneous Raman signal collected evanescently by silicon nitride slot waveguides," in *Proc. CLEO, Sci. Innov.*, May 2015, pp. 1–2, Paper. STh4H.3.

[14] D. M. Kita, J. Michon, S. G. Johnson, and J. Hu, "Are slot and sub-wavelength grating waveguides better than strip waveguides for sensing?" *Optica*, vol. 5, no. 9, pp. 1046–1054, 2018.

[15] Q. Cao, J. Feng, H. Lu, H. Zhang, F. Zhang, and H. Zeng, "Surface-enhanced Raman scattering using nanoporous gold on suspended silicon nitride waveguides," *Opt. Exp.*, vol. 26, no. 19, pp. 24614–24620, Sep. 2018.

[16] P. C. Wuytens, A. G. Skirtach, and R. Baets, "On-chip surface-enhanced Raman spectroscopy using nanosphere-lithography patterned antennas on silicon nitride waveguides," *Opt. Express*, vol. 25, no. 11, pp. 12926–12934, May 2017.

[17] A. Raza *et al.*, "ALD assisted nanoplasmonic slot waveguide for on-chip enhanced Raman spectroscopy," *APL Photon.*, vol. 3, no. 11, Oct. 2018, Art. no. 116105.

[18] Y. Zhou *et al.*, "Human brain cancer studied by resonance Raman spectroscopy," *J. Biomed. Opt.*, vol. 17, no. 11, Nov. 2012, Art. no. 116021.

[19] C.-H. Liu *et al.*, "Resonance Raman and Raman spectroscopy for breast cancer detection," *Technol. Cancer Res. Treat.*, vol. 12, no. 4, pp. 371–382, Aug. 2013.

[20] K. Schmitt, K. Oehse, G. Sulz, and C. Hoffmann, "Evanescent field sensors based on tantalum pentoxide waveguides—A review," *Sensors*, vol. 8, no. 2, pp. 711–738, 2008.

[21] B. S. Ahluwalia, A. Z. Subramanian, O. G. Hellso, N. M. B. Perney, N. P. Sessions, and J. S. Wilkinson, "Fabrication of submicrometer high refractive index tantalum pentoxide waveguides for optical propulsion of microparticles," *IEEE Photon. Technol. Lett.*, vol. 21, no. 19, pp. 1408–1410, Oct. 12, 2009.

[22] C. Joseph, P. Bourson, and M. D. Fontana, "Amorphous to crystalline transformation in Ta_2O_5 studied by Raman spectroscopy," *J. Raman Spectrosc.*, vol. 43, no. 8, pp. 1146–1150, Aug. 2012.

[23] S. P. S. Porto, P. A. Fleury, and T. C. Damen, "Raman spectra of TiO_2, MgF_2, ZnF_2, FeF_2, and MnF_2," *Phys. Rev. J. Arch.*, vol. 154, no. 2, pp. 522–526, Feb. 1967.

[24] D. Lin-Vien, N. B. Colthup, W. G. Fateley, and J. G. Grasselli, *The Handbook of Infrared and Raman Characteristic Frequencies of Organic Molecules*. Amsterdam, The Netherlands: Elsevier, 1991.

[25] J. B. Wallach, *Interpretation of Diagnostic Tests*. Philadelphia, PA, USA: Lippincott Williams & Wilkins, 2007.

[26] R. Diekmann *et al.*, "Chip-based wide field-of-view nanoscopy," *Nature Photon.*, vol. 11, no. 5, pp. 322–328, May 2017.

[27] Ø. I. Helle, D. A. Coucheron, J.-C. Tinguely, C. I. Øie, and B. S. Ahluwalia, "Nanoscopy on-a-chip: super-resolution imaging on the millimeter scale," *Opt. Express*, vol. 27, no. 5, pp. 6700–6710, Mar. 2019.